Scanning Tunneling Microscopy of Ethylated Si(111) Surfaces Prepared by a Chlorination/Alkylation Process

Hongbin Yu, Lauren J. Webb, Santiago D. Solares, Peigen Cao, William A. Goddard III,* James R. Heath,* and Nathan S. Lewis*

Division of Chemistry and Chemical Engineering, Beckman Institute and Kavli Nanoscience Institute, 127−72, Noyes Laboratory, California Institute of Technology, Pasadena, California 91125

Received: June 12, 2006; In Final Form: August 2, 2006

Scanning tunneling microscopy (STM) and computational modeling have been used to study the structure of ethyl-terminated Si(111) surfaces. The ethyl-terminated surface was prepared by treating the H-terminated Si(111) surface with PCl_5 to form a Cl-terminated Si(111) surface with subsequent exposure to C_2H_5MgCl in tetrahydrofuran to produce an alkylated Si(111) surface. The STM data at 77 K revealed local, close-packed, and relatively ordered regions with a nearest-neighbor spacing of 0.38 nm as well as disordered regions. The average spot density corresponded to ≈85% of the density of Si atop sites on an unreconstructed Si(111) surface. Molecular dynamics simulations of a Si(111) surface randomly populated with ethyl groups to a total coverage of ≈80% confirmed that the ethyl-terminated Si(111) surface, in theory, can assume reasonable packing arrangements to accommodate such a high surface coverage, which could be produced by an exoergic surface functionalization route such as the two-step chlorination/alkylation process. Hence, it is possible to consistently interpret the STM data within a model suggested by recent X-ray photoelectron spectroscopic data and infrared absorption data, which indicate that the two-step halogenation/alkylation method can provide a relatively high coverage of ethyl groups on Si(111) surfaces.

I. Introduction

Functionalization with covalently bonded organic reagents has attracted interest as a method to manipulate the chemical and electrical properties of Si surfaces.[1−5] Alkyl passivated Si(111) surfaces that are prepared through a two-step chlorination/alkylation route[6−8] have shown low charge-carrier surface recombination velocities, oxidation resistance in air and during anodic current flow in electrochemical cells,[9] and a number of other interesting chemical and electronic properties.[6] An advantage of the halogenation/alkylation method is that it offers a facile route to the preparation of oxide-free Si(111) surfaces that are terminated with methyl groups that on steric grounds are expected to provide the most complete coverage of Si atop sites of all the saturated, straight-chain alkyls.[10] X-ray photoelectron spectroscopy,[11] low-energy electron diffraction (LEED),[11] infrared absorption,[12] and scanning tunneling microscopy (STM) studies[13] have confirmed that the CH_3-terminated Si(111) surface adopts a highly ordered unreconstructed 1×1 structure in which each atop silicon atom is bonded to a methyl group oriented normal to the surface plane.

The distance between Si atop sites on an unreconstructed 1×1 Si(111) surface is 3.8 Å, whereas the van der Waals diameter of a methyl group is 2.3 Å, and the van der Waals diameter of methylene groups in alkane chains has been estimated to be 4.5−5.0 Å.[10] Hence, for alkyl groups other than methyl, steric interactions are expected to limit the coverage of Si atop sites bonded to the alkyl groups.[14,15] In this work, STM has been used to characterize the ethylated Si(111) surface that was prepared using the two-step chlorination/alkylation approach. These data are consistent with a model in which Si(111) can be alkylated in a highly exoergic reaction to form a high coverage (≈80%) of ethyl groups, and can indicate that the resultant surface structure has ordered regions consistent with ethylation of the atop sites of an unreconstructed Si(111) 1×1 surface as well as less ordered regions.

II. Experimental Section

Silicon surfaces were (111)-oriented, Sb-doped, 0.005−0.02 Ω-cm resistivity, n-type Si wafers having a miscut error of ±0.5°. The samples were cleaned and oxidized for 5 min at 80° C in a solution of 1:1:5 (vol) 30% H_2O_2/30% NH_3/H_2O and then were etched for 15 min in 40% NH_4F(aq). This etching method has been demonstrated to produce H-termination with large atomically flat terraces on the Si(111) surface.[13] Chlorination was performed by exposure of the samples to a solution of PCl_5 in chlorobenzene.[8,16] A small amount of benzoyl peroxide was added to initiate the reaction, and the samples were heated at 90−100 °C for 45 min. The surfaces were removed from solution, rinsed with tetrahydrofuran (THF) and CH_3OH, and then dried under a stream of N_2(g). To form the C_2H_5−Si(111) surface, the resulting Cl-terminated surfaces were exposed for 3−5 h to 3.0 M C_2H_5MgCl in refluxing THF. The samples were rinsed with THF and CH_3OH followed by sonication for 5 min in CH_3OH and then in CH_3CN. The samples were dried under a stream of N_2(g), mounted onto a sample stage, and quickly introduced into the ultra-high vacuum (UHV) system of an Omicron low-temperature UHV STM. Images were obtained using etched or mechanically cut Pt/Ir STM tips. Alignment of the images with respect to the flat at the edge of the wafer allowed alignment of the lattice vectors of the crystal with the STM images.

* To whom correspondence should be addressed. E-mail: (N.S.L.) nslewis@its.caltech.edu; (J.R.H.) heath@caltech.edu; (W.A.G.) wag@wag.caltech.edu.

10.1021/jp063655g CCC: $33.50
Published on Web 11/09/2006

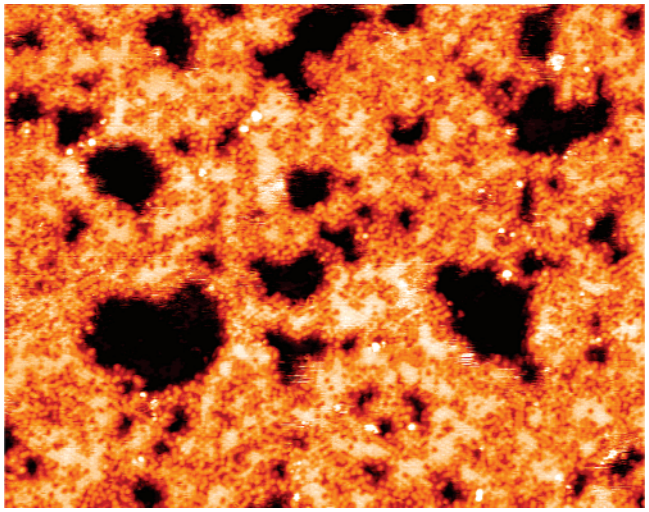

Figure 1. Large scale constant current (0.05 nA; sample at −3 V vs tip) STM image at 77 K of the ethyl-terminated Si(111) surface prepared through chlorination/alkylation wet chemistry steps. Image size: 47.5 × 37.5 nm. Light color corresponds to higher regions in topography. Quasi-ordered close-packing exists in these regions. The intermediate (orange) color represents lower regions where individual spots can be seen, but no apparent order exists. Dark regions are at least one silicon double-step lower in height.

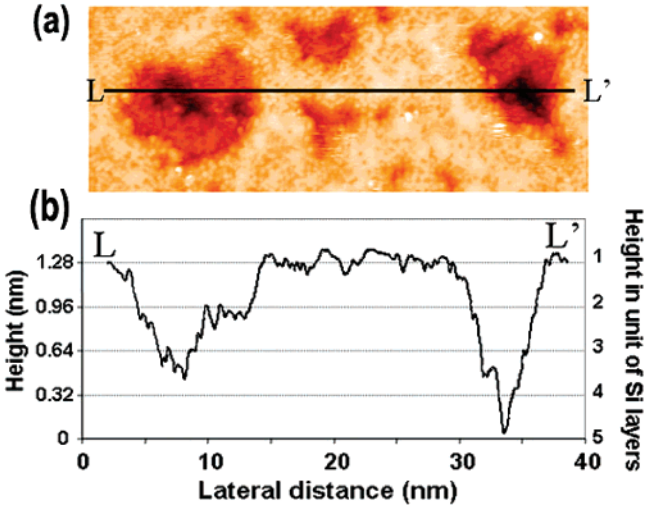

Figure 2. (a) A 37.5 × 12.5 nm image of ethylated-Si(111) revealing the surface topology. (b) The line profile (*LL′* in (a)) indicates etch pits that are multiple silicon layers deep (each silicon double layer height is 0.313 nm). On a given layer, there are further height variations on the scale of 0.1−0.2 nm.

III. Results

A. STM Data. Figure 1 shows a large area STM image at 77 K of an ethylated Si(111) surface. In this image, different heights are represented by a color scale with light representing higher regions and dark representing lower regions. The lighter regions have quasi-ordered close packing (not visible in this large-scale image); the intermediate orange color represents lower regions where individual spots with less ordering are observed. The orange and light-colored regions are on the top silicon surface plane. The dark regions are at least one silicon double-layer step lower in height but still display atomic level ordering of the surface-bound alkyl groups (see Figure 2). The pits are likely the result of silicon etching during the chlorination/alkylation process, because such features are not observed after the preparation of H-terminated Si(111) using NH_4F(aq).[13] Figure 2 depicts an expanded view of a region from part of the image of Figure 1, but with the contrast adjusted such that the difference between atomic layers can be seen more clearly. The line profile displayed in Figure 2b, which was taken along *LL′* in Figure 2a, reveals these etched pits.

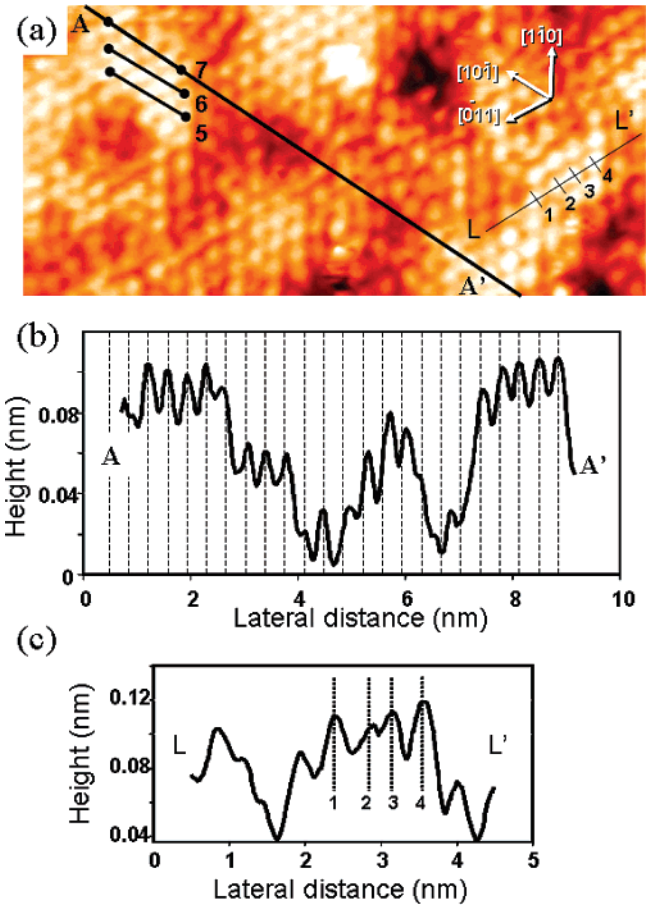

Figure 3. Morphology and molecular structures on ethyl-Si(111). (a) Molecular resolution STM image of top layer on ethyl-Si(111) taken at 77 K in constant current mode with the sample biased at −3 V and the tunneling current set at 0.05 nA. Image size: 10 × 4.7 nm. (b) Line profile taken in (a) along *AA′* shows the corrugation on the surface. Dashed lines with a periodicity of 0.38 nm are superimposed on the profile to illustrate that the distance between neighboring spots in the ordered region is close to the characteristic distance of the unreconstructed Si(111) 1 × 1 structure. (c) The line profile taken in (a) along *LL′* reveals that even the "ordered" regions are characterized by significant disorder, although the average spacing between the adjacent lines 1−4 is 0.38 nm.

The top layer of the Si(111) surface that is shown in Figure 2 exhibited the full extent of the interesting features observed during this study. Thus, we focus on a high-resolution image of this layer in Figure 3a. This image and the line profile *A*−*A′* (Figure 3b) reveal relatively ordered regions on this surface. The image of Figure 3a exhibits a total of 312 spots within an area that could accommodate 366 surface Si atoms for a spot density of 85% relative to the density of Si atop sites on an unreconstructed 1 × 1 Si(111) surface. Dashed lines with a periodicity of 0.38 nm are superimposed on the profile of Figure 3b to illustrate that the distance between neighboring spots was approximately 0.38 nm, which is the characteristic distance between the nearest neighbor Si atop surface atoms on an unreconstructed Si(111) 1 × 1 surface. These data demonstrate that regions of close-packed molecular structure exist on the surface. Between these ordered regions, other regions are evident that are lower in height and have characteristic next neighbor

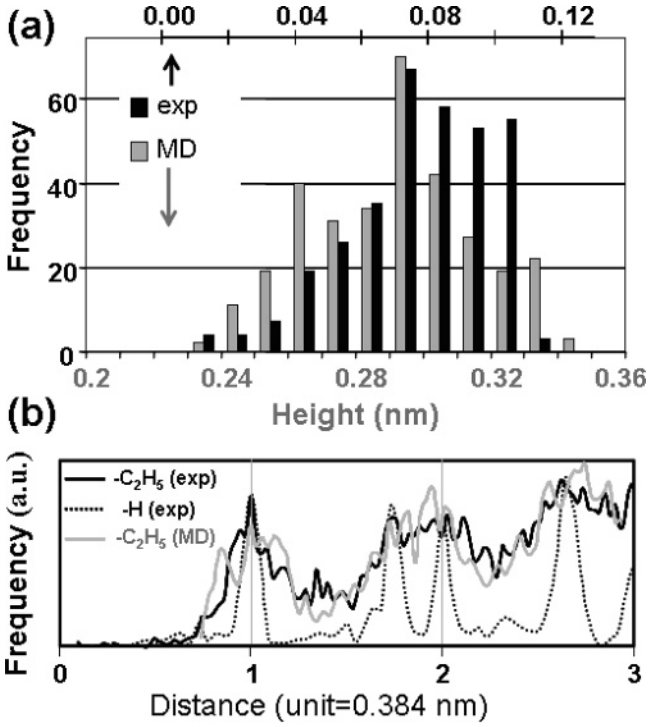

Figure 4. (a) Experimental (black) and MD-generated (gray) height variations of ethylated Si(111). The experimental height distribution was generated by measuring the local maximum of each bright spot shown in panel 3a. (b) Pair-distance distribution on ethyl-terminated Si(111) (solid line) and H-terminated Si(111) (dashed line). The data were obtained by analyzing the bright spots in high-resolution STM images collected from the surfaces at 77 K and from MD simulations on a 20 × 20 unit cell with 80% ethyl coverage. The H-terminated surface reflects the ideal 1 × 1 surface structure of the underlying silicon lattice. The ethyl-terminated distribution function is indicative of significant disorder in the ethyl packing.

distances that are generally not equal to 0.38 nm (cf., the middle part of the line profile in Figure 3b).

To quantify further the observed height variations, the frequencies of the measured heights of the molecular features in Figure 3a were analyzed statistically (Figure 4a, black). In this analysis, the local maximum height representing each feature was identified and was used for the counting. As shown in Figure 4a, the height variation on the surface was in the range of 0.1 nm, implying that all of the local maxima originated from the structure of the top Si layer.

Close inspection of the measured structure within the most ordered regions revealed that even those areas are not perfectly ordered. The line profile $L-L'$, which is shown in Figure 3c, is taken through one of these ordered regions. The total distance between the four adjacent maxima is 1.14 nm, which is equal to 3 × 0.38 nm. However, distances between the individual maxima varied significantly. They were measured to be 0.47, 0.28, and 0.40 nm for distances 1−2, 2−3, and 3−4, respectively.

Lateral distance variations within the close-packed region also are evidenced by comparing lines 5, 6, and 7 that also are superimposed on Figure 3a. These lines are drawn through the center of separate spot arrays to guide the eye. The distance between lines 5 and 6 (0.28 nm) is smaller than that between lines 6 and 7 (0.36 nm). Similar variations were observed for different STM scan directions and across other "ordered" regions of the surface, which indicates that these experimental results are not an artifact of the measurement technique.

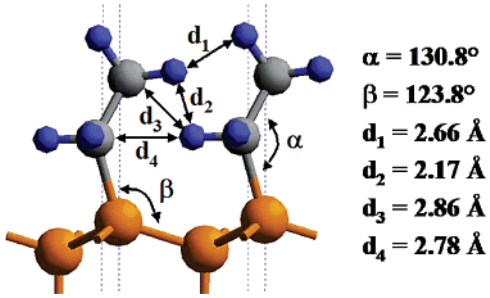

Figure 5. Atomistic model showing two adjacent unit cells of the 1 × 1 C_2H_5−Si(111) surface and the most relevant bond angles (α and β) and nonbond distances (d_1, d_2, d_3, and d_4) that were obtained from quantum mechanics calculations. The color code is blue = hydrogen, gray = carbon, and orange = silicon.

As displayed in Figure 4b, a radial distribution function was constructed based on the bright spots in the image of Figure 3a. For comparison, the same analysis was carried out on an STM image taken from a highly ordered H-terminated Si(111) surface. The H atoms on this surface are well-known to be attached directly to the atop silicon atoms on Si(111) with the Si−H bonds directed normal to the surface.[17] This distribution is thus a representation of the underlying unreconstructed 1 × 1 Si lattice. The lateral distances in Figure 4b have been normalized to the 0.38 nm Si nearest neighbor distance. The distribution function of the C_2H_5-terminated Si(111) surface demonstrates that the pair−pair distances of overlayer molecular groups roughly followed the same pattern observed on the H-terminated surface with peaks at distances representing successive nearest-neighbors. However, significant amplitude also is observed for pair−pair correlations at distances other than those expected for the unreconstructed surface.

B. Theory and Modeling. Periodic quantum mechanics (QM) calculations (SeqQuest software,[18] Sandia National Labs., Albuquerque, NM) using the PBE[19] flavor of density functional theory (DFT) were performed to calculate the geometry of the C_2H_5−Si(111) surface at 100% coverage. The calculations were made on a 1 × 1 unit cell that consisted of six bulk silicon atoms, a hydrogen atom terminating the bottom surface, and an ethyl group terminating the top surface. These results showed that the ethylated surface is quite significantly strained with large bond angles and short nonbond distances. Figure 5 shows the equilibrium C−C−Si and C−Si−Si bond angles, which were found to be 130.8° and 123.8°, respectively, and both were appreciably larger than the tetrahedral value of 109.4°. The nonbond H- - -H distances were calculated to be as low as 2.17 Å, which was much shorter than calculated for a fully methyl-terminated Si(111) surface (2.33 Å) or for the shortest distances in polyethylene (2.51 Å). Figure 6 compares the strain energies for the structures of Si(111)−CH_3 and Si(111)−C_2H_5, which shows that the extra strain in the ethylated surface is ∼9 kcal/mol per substituent.

PBE DFT calculations were performed for coverages of 25, 50, and 75% of the 2 × 2 Si(111)−CH_3 and Si(111)−C_2H_5 unit cells, for 67% of the 3 × 3 cell, and for 100% of the 1 × 1 cell. The sites not covered with methyl or ethyl were terminated with hydrogen. In each case, the average bond energy of the appropriate functional group (methyl or ethyl) was compared to its bond energy on a Si(111) surface site of a hydrogen-passivated Si_{10} cluster. The bond to this cluster was taken as the reference and was assigned zero strain. The average strain energy per ethyl group was ∼20% higher than for the methyl case up to 50% coverage (Figure 6). Between 67 and 75% coverage, the strain energy increases dramatically (by 80%)

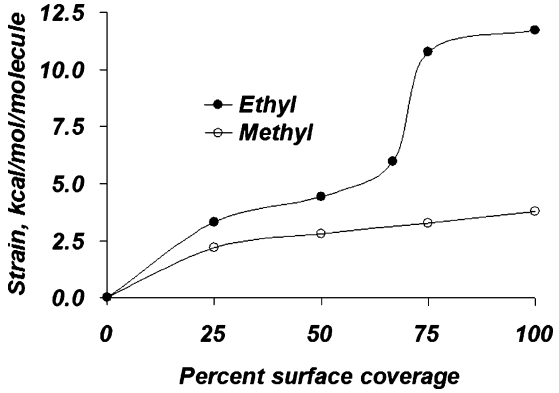

Figure 6. Strain energy per occupied surface site for quantum mechanics calculations for Si(111)−CH_3 and Si(111)−C_2H_5 as a function of surface coverage from quantum mechanics calculations. The sites not occupied with ethyl or methyl were terminated with hydrogen atoms. The reference is an ethyl or methyl group bonded to a 1 × 1 site cluster with no nearest-neighbors.

for ethyl, but not for methyl. At 75% coverage, to pack into the cell, the C−C−Si angle of the ethyl must increase significantly (∼20°) and becomes nearly vertical. At 100% coverage, the amount of strain is three times greater for ethyl than for methyl.

The change in free energy and enthalpy for the Grignard reaction [Cl−Si(111) + C_2H_5−Mg−Cl → C_2H_5−Si(111) + $MgCl_2$ in THF] was calculated using nonperiodic QM (Jaguar software, Schrödinger, Portland, OR) using the B3LYP flavor of DFT with 631G** basis sets. Solvation effects were included using the Poisson−Boltzmann model (assuming a dielectric constant of 7.52 and a solvent radius of 2.526 Å for THF). The Si(111) sites were modeled as Si−$(SiH_3)_3$ clusters with a single dangling bond attached to Cl or C_2H_5. This leads to calculated values of $\Delta G^{298} = -47.1$ kcal/mol and $\Delta H^{298} = -48.6$ kcal/mol for the Grignard reaction, which were much greater than the 12 kcal/mol of strain energy calculated for 100% ethyl coverage. However, the alkylation process is probably limited by the steric interactions near the transition state, which reduces the maximum coverage to ∼80%.

Because the C_2H_5−Si(111) surfaces prepared experimentally contain etch pits and step edges and because ≈16% of the surface sites are located on the edges, strain energy calculations also were performed on two-dimensional (2D), periodic unit cells containing steps. We previously have demonstrated the thermodynamic feasibility of the emergence of a stacking fault[20] on the terraces of the CH_3−Si (111) surface, which would lead to step edge terminations having the same structure as the reconstructed <$\bar{1}\bar{1}$2> step edge[21] (see Figure 7). This results from Pauli principle (steric) repulsions between −CH_3 groups on the steep edge and those on the nonfaulted terrace surface and in the pits. Such steric repulsions for the C_2H_5−Si(111) surface should be at least as large as those for the CH_3-terminated surface. Hence, calculations were performed on the unit cell shown in Figure 7 in which every sixth site is located on a reconstructed <$\bar{1}\bar{1}$2> step edge for surface coverages of 100% and 83% (with remaining sites occupied by hydrogen atoms instead of ethyl groups). The ≈83% coverage corresponds approximately to the 85% surface coverage determined experimentally from XPS[22] and infrared[12] measurements and is consistent with an interpretation in which the STM spots observed herein arise from the surface-bound ethyl groups. Because the sites at the step edges are farther from their neighbors than those on the perfect surface, lower strain is produced. Thus, the hydrogen-terminated site was selected to be the one farthest from the step edge (Figure 7). The result is that that the presence of a step edge in the unit cell reduces the average strain energy per ethyl molecule from ∼11.8 to ∼9.4 kcal/mol for 100% coverage and from ∼10.7 to ∼7.5 kcal/mol for 83% coverage. Thus, the experimental surface is expected to have ∼7.5 kcal/mol of strain per site.

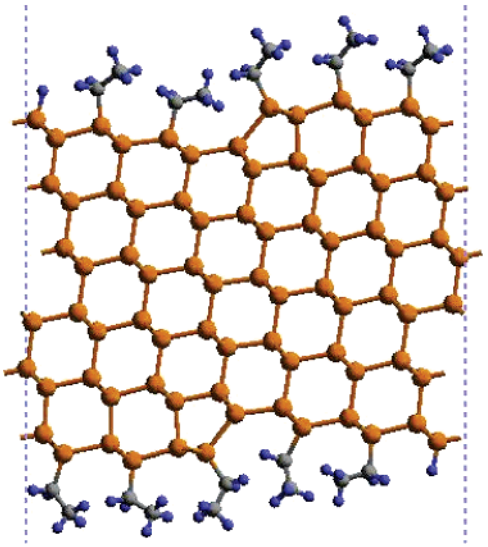

Figure 7. Unit cell used for the strain energy calculation in the presence of surface step edges for 83% ethyl coverage. The unit cell was obtained by cutting the silicon crystal along the ⟨668⟩ plane and adding ethyl groups at all the surface sites except the one farthest from the edge, which is occupied with hydrogen. This structure contains six surface sites on each side (including one on the step edge) and an infinite <$\bar{1}\bar{1}$2> step. The structure with 100% ethyl coverage is similar but has all sites occupied with ethyl.

To quantify further the height variations observed in Figure 3 and to validate whether the interpretation of ∼85% coverage of the Si(111) atop sites with ethyl is reasonable, molecular dynamics (MD) calculations were performed on a randomly populated 20 × 20 Si(111)−C_2H_5 unit cell with 80% coverage with all sites not occupied with ethyl groups terminated with hydrogen. These calculations used the Cerius2 software (Accelrys, San Diego, CA) with previously reported force-field parameters for silicon[23] and hydrocarbons[24] but with the H−C−Si−Si torsional parameter adjusted to 2.945 kcal/mol based on DFT (SeqQuest) calculations. From those simulations, two predictions were extracted that could then be directly compared with the data of Figure 3. The first involved comparison of a histogram of the frequency of the measured heights of the molecular features seen in Figure 3a, as shown in Figure 4a. For the MD simulation, the height variation was based on the position of the top carbon atom (C2) of the ethyl molecule, which can rotate around the 1 × 1 site and also can be displaced horizontally and vertically through changes in the Si−C−C and Si−Si−C bond angles. In the close-packed regions with nearly complete surface coverage, adjacent ethyl molecules have similar orientation that results in C2 arrangements that resemble the 1 × 1 unreconstructed surface sites. In the regions that contain hydrogen-terminated surface sites (i.e., where the local ethyl coverage is less than 100%), the ethyl molecules can rotate and stretch to minimize the repulsions with their neighbors such that their C2 atoms can be oriented in any direction and not necessarily resembling the 1 × 1 surface sites. The comparison of the radial distribution functions between experiment and theory is depicted in Figure 4b. In general, the agreement is quite good.

IV. Discussion

The STM data show extensive regions of quasi-order with a spot density that corresponds to ≈85% of the density of atop sites on an unreconstructed Si(111) surface. By themsevles, the STM data do not allow an unambiguous assignment of the spots to alkyls or to putative surface Si−H bonds that might be introduced during the Grignard quenching and workup steps.[10,12] STM data on surfaces that only are partially covered with alkyls might be helpful in this regard. However, stable tunneling conditions were not obtained on surfaces that had been treated for relatively short times (1 h) in the functionalization process, whereas surfaces that had been alkylated for 3 h displayed regions that were similar in coverage and behavior to those depicted in Figures 1−4.

Surface sensitive, soft X-ray photoelectron spectroscopy (SXPS) has shown that ethylation of Si using the two-step chlorination/alkylation method produces no detectable Si oxide and leaves no elements on the surface other than Si, C, and O.[10] A high-resolution SXPS scan of the ethyl-terminated surface in the C 1s region has revealed a low-energy emission ascribable to carbon bonded to the more electropositive Si.[11,22] Quantitative analysis of the ratio of this emission, C_{Si}, to the area of the Si 2p emission indicates that when $-C_2H_5$ is used as the terminating alkyl group then ≈80% of the Si surface atop atoms are bonded to carbon.[22] Infrared absorption spectroscopy[12] and X-ray photoelectron spectroscopy[22] are thus consistent with the hypothesis that Si−H bonds terminate most of the nonalkylated Si surface sites.[10,12,22]

Scanning tunneling spectroscopy[25] and ultraviolet photoelectron spectroscopy (UPS)[11] indicate no detectable molecular orbital states near the Fermi level of such surfaces, and thus relatively few dangling bonds are present on the surface. The bias used for the STM imaging experiments was −3 V. Under such conditions, geometric factors rather than electronic ones, are likely to dominate the surface images because the alkyl groups that are bonded to the silicon surface have no molecular orbital levels within the applied voltage window.[11,25,26] On the basis of the height difference between an ethyl group and a H atom, it is likely that no H-terminated sites are imaged by STM because they would be shadowed by surrounding ethyl groups. Thus, the bright features in the STM images can consistently be assigned to some part of the top methyl group of the surface-bound ethyl groups.

A model which assumes that each spot is associated with an ethyl group would indicate that ≈85% of the unreconstructed Si(111) surface is terminated with ethyl groups. Including the uncertainty at the image boundary to assign possible surface Si atom sites, the coverage of ethyl groups would be between 75 and 90% of a full surface monolayer. This value is consistent with Fourier transform IR (FTIR) and XPS studies of the ethyl-terminated surface, which indicate that the ethyl groups are bonded to ∼80% of available surface Si(111) atoms.[12,22]

For small chains such as ethyl, relatively little strain is introduced at a periodic coverage of 66% of the Si atop sites. Defects such as etch pits can allow still further increases in coverage of alkyl groups while introducing relatively little strain into the alkyl overlayer. In addition, the highly favorable thermodynamics for the reaction of R−MgCl with Cl−Si can allow the introduction of significant strain energy into the resulting surface, and thus produces still higher coverages of alkyls on the Si(111) surface. Hence, the observed STM images can be understood in terms of the factors controlling formation of the alkylated surface using the two-step chlorination/alkylation method and are consistent with a model suggested by the XPS and IR data in which a relatively high coverage of ethyl groups is obtained using the exoergic, two-step, chlorination/ethylation reaction process.

V. Conclusions

STM images of C_2H_5-terminated Si(111) reveals local, close-packed, and relatively ordered regions with a nearest-neighbor spacing close to the value of 0.38 nm that is expected for an unreconstructed surface but also reveals many disordered regions. The average spot density corresponded to ≈85% of the density of Si atop sites on an unreconstructed Si(111) surface. The data are consistent with theoretical models for the bonding, structure, and packing of ethyl-terminated Si(111) as obtained from molecular dynamics and quantum mechanics calculations in which the free energy of the reaction and the presence of defect sites on the surface are considered, respectively, with respect to contributions to produce and relieve bond strain on the ethyl-terminated Si(111) surface. The data are consistent with an interpretation in which relatively high coverages of ethyl groups can be obtained on Si(111) surfaces prepared by the two-step halogenation/alkylation method in accord with recent X-ray photoelectron spectroscopic data and infrared absorption data on such surfaces.

Acknowledgment. The authors acknowledge the National Science Foundation, Grants CHE-0604894 (N.S.L.) and NSF-CCF-05204490, the MARCO Materials Structures and Devices Focus Center (J.R.H. and W.A.G), and the Department of Energy for support of this research. L.J.W. thanks the NSF for a graduate fellowship.

References and Notes

(1) Bunimovitch, Y. L.; Ge, G.; Beverly, K. C.; Ries, R. S.; Hood, L.; Heath, J. R. *Langmuir* **2004**, *20*, 10630−10638.
(2) Buriak, J. M. *Chem. Rev.* **2002**, *102*, 1271−1308.
(3) Bent, S. F. *Surf. Sci.* **2002**, *500*, 879−903.
(4) Wolkow, R. A. *Annu. Rev. Phys. Chem.* **1999**, *50*, 413−441.
(5) Wayner, D. D. M.; Wolkow, R. A. *J. Chem. Soc., Perkin Trans. 2* **2002**, *2*, 23−34.
(6) Bansal, A.; Lewis, N. S. *J. Phys. Chem. B* **1998**, *102*, 1067−1070.
(7) Royea, W. J.; Juang, A.; Lewis, N. S. *Appl. Phys. Lett.* **2000**, *77*, 1988−1990.
(8) Webb, L. J.; Lewis, N. S. *J. Phys. Chem. B* **2003**, *107*, 5404−5412.
(9) Bansal, A.; Lewis, N. S. *J. Phys. Chem. B* **1998**, *102*, 4058−4060.
(10) Webb, L. J.; Nemanick, E. J.; Biteen, J. S.; Knapp, D. W.; Michalak, D. J.; Traub, M. C.; Chan, A. S. Y.; Brunschwig, B. S.; Lewis, N. S. *J. Phys. Chem. B* **2005**, *109*, 3930−3937.
(11) Hunger, R.; Fritsche, R.; Jaeckel, B.; Jaegermann, W.; Webb, L. J.; Lewis, N. S. *Phys. Rev. B.* **2005**, *72*, 045317.
(12) Webb, L. J.; Rivillon, S.; Michalak, D. J.; Chabal, Y. J.; Lewis, N. S. *J. Phys. Chem. B* **2006**, *110*, 7349−7356.
(13) Yu, H.; Webb, L. J.; Ries, R. S.; Solares, S. D.; Goddard, W. A.; Heath, J. R.; Lewis, N. S. *J. Phys. Chem. B* **2005**, *109*, 671−674.
(14) Sieval, A. B.; van den Hout, B.; Sudholter, E. J. R. *Langmuir* **2000**, *16*, 2987−2990.
(15) Sieval, A. B.; van den Hout, B.; Zuilhof, H.; Sudholter, E. J. R. *Langmuir* **2001**, *17*, 2172−2181.
(16) Bansal, A.; Li, X.; Yi, S. I.; Weinberg, W. H.; Lewis, N. S. *J. Phys. Chem. B* **2001**, *105*, 10266−10277.
(17) Hines, M. A. *Annu. Rev. Phys. Chem.* **2003**, *54*, 29−56.
(18) Schultz, P. A. SeqQuest Electronic Structure Code. http://dft.sandia.gov/Quest/, Sandia National Laboratory, Albuquerque, NM.
(19) Perdew, J. P.; Burke, K.; Ernzerhof, M. *Phys. Rev. Lett.* **1996**, *77*, 3865−3868.
(20) Solares, S. D.; Yu, H.; Webb, L. J.; Lewis, N. S.; Heath, J. R.; Goddard, W. A. *J. Am. Chem. Soc.* **2006**, *128*, 3850−3851.
(21) Itchkawitz, B. S.; McEllistrem, M. T.; Boland, J. J. *Phys. Rev. Lett.* **1997**, *78*, 98−101.
(22) Nemanick, E. J.; Hurley, P. T.; Brunschwig, B. S.; Lewis, N. S. **2006**, *J. Phys. Chem. B*, in press.
(23) Shapiro, I. R.; Solares, S. D.; Esplandiu, M. J.; Wade, L. A.; Goddard, W. A.; Collier, C. P. *J. Phys. Chem. B* **2004**, *108*, 13613−13618.

(24) Mayo, S. L.; Olafson, B. D.; Goddard, W. A. *J. Phys. Chem.* **1990**, *94*, 8897−8909.
(25) Yu, H.; Webb, L. J.; Lewis, N. S.; Heath, J. R. *Appl. Phys. Lett*. **2006**, *88*, 252111.
(26) Miyadera, T.; Koma, A.; Shimada, T. *Surf. Sci*. **2003**, *526*, 177−183.